

Capillary Fluctuations and Film–Height–Dependent Surface Tension of an Adsorbed Liquid Film

Luis G. MacDowell¹, Jorge Benet¹ and Nebil A. Katcho²

¹*Departamento de Química Física, Facultad de Química, Universidad Complutense de Madrid, 28040 Madrid, Spain*

²*LITEN, CEA-Grenoble, 17 rue des Martyrs, 38054 Grenoble Cedex 9, France.*

Abstract

Our understanding of both structure and dynamics of adsorbed liquids heavily relies on the capillary wave Hamiltonian, but a thorough test of this model is still lacking. Here we study the capillary wave fluctuations of a liquid film with short range forces adsorbed on a solid exhibiting van der Waals interactions. We show for the first time that the measured capillary wave spectrum right above the first order wetting transition provides an interface potential consistent with independent calculations from thermodynamic integration. However, the surface tension exhibits an oscillatory film thick dependence which reveals a hitherto unnoticed capillary wave broadening mechanism beyond mere interfacial displacements.

State of the art nanotechnology allows for the synthesis of intricate devices, with microchannels, grooves and minute containers that offer a great number of potential applications.[1] Taking advantage of this synthetic technology also requires a thorough understanding and control of the fluid behavior within the structured materials.[2] In surface physics, most of our understanding of adsorbed fluids relies on the concept of *interface potential*, $g(\ell)$, the (surface) free energy of a flat adsorbed liquid film of height ℓ above the substrate.[3, 4] For practical applications, however, we expect that adsorbed condensates within a device will display a complex geometry which can no longer be described by a simple scalar film height, but rather, by a complex film profile $\ell(\mathbf{x})$ which is now a function of the position \mathbf{x} on the plane of the substrate. Our understanding of such situations heavily relies on the phenomenological capillary wave Hamiltonian, $H[\ell]$ (CWH), a functional of the film profile which assumes a free energy $g(\ell(\mathbf{x}))$ locally, but includes extra contributions due to bending of the interface via the liquid–vapor surface tension, γ_∞ :[5, 6]

$$H[\ell] = \int d\mathbf{x} \left(g(\ell(\mathbf{x})) + \gamma_\infty \sqrt{1 + (\nabla\ell)^2} \right) \quad (1)$$

The equation above is at the heart of most theoretical accounts of surface phenomena, including, renormalization group analysis of wetting transitions [7], the study of droplet profiles [8], or the calculation of line tensions [9].

The validity of the CWH, however, very much depends on dimensionality and range of the intermolecular forces considered. In two dimensions, the CWH may be recovered exactly from the Ising model.[10] For three dimensions and short–range forces, on the other hand, it has been long recognized that Eq. (1) cannot be derived bottom–up from a microscopic Landau–Ginzburg–Wilson functional (LGW) even for a flat substrate.[11, 12] Fisher and Jin argued that the form of Eq. (1) may be retained provided one employs a modified local interface

potential and a position dependent surface tension.[11] For the short–range critical wetting transition, however, Parry and collaborators have shown that Eq. (1) has to be discarded altogether in favor of a nonlocal functional of $\ell(\mathbf{x})$, which does recover the result of Fisher and Jin in the case of complete wetting.[12] Surprisingly, the very practically relevant case of a flat substrate subject to long–range wall–fluid interactions exhibiting a first order wetting transition has received much less attention.[13] It is this problem that we would like to address in this Letter.

A simple means of testing Eq. (1) is to consider a film adsorbed on a flat substrate.[14, 15] Thermal excitations of the otherwise planar film of lateral area A , produce capillary waves, with amplitudes that are damped by the interface potential.[6] Expanding the film profile in Fourier modes, $\ell(\mathbf{x}) = \sum_{\mathbf{q}} \ell_{\mathbf{q}} e^{i\mathbf{q}\mathbf{x}}$, allows us to calculate a capillary wave spectrum (CWS). In the regime of Gaussian fluctuations, the CWS expected from Eq. (1) is:[16–18]

$$\frac{k_B T}{A < |\ell_{\mathbf{q}}|^2 >} = g''_{cws} + \gamma_{cws} q^2 + \kappa_{cws} q^4 \quad (2)$$

where k_B is the Boltzmann constant, T is the temperature and the angle brackets denote a thermal average; while g''_{cws} , γ_{cws} and κ_{cws} are the first few coefficients of an expansion in powers of \mathbf{q} . Even for Gaussian fluctuations, the relation between the coefficients of Eq. (1) and Eq. (2) may not be trivial. In fact, Eq. (2) provides at best the renormalized interface potential and surface tensions. In our three–dimensional system subject to long–range interactions, however, we are safely above the upper critical dimension, and do not expect significant renormalization. The first two terms in the right–hand side, with $g''_{cws} = g''(\ell)$ and $\gamma_{cws} = \gamma_\infty$ then follow from the classical model of Eq. (1), and may be measured independently, while an extra term of order q^4 is known to arise already for free liquid–vapor interfaces in the absence of an external field.[17, 18]

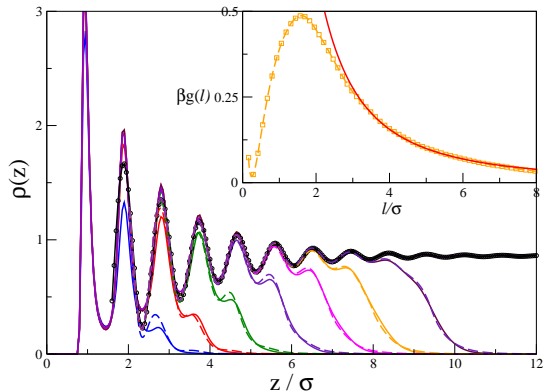


FIG. 1. Density profiles for adsorbed layers of thickness ℓ of (full lines, from left to right) 1.9, 3.0, 4.1, 5.3, 6.5, 7.3 and 8.5σ . The symbols depict the function $A_w \cos(k_o z + \theta) \exp(-b_o z)$ with k_o and b_l obtained from the bulk correlation function, and A_w , θ obtained from a fit to an adsorbed layer of thickness ℓ ca. 35σ . Dashed lines are predictions from the superposition model, Eq. (6). Inset: Interface potential as a function of average film thickness, ℓ (symbols). Expectations from the Hamaker model are shown as a dark line.

Here we show for the first time that g''_{cws} as obtained from the CWS, is fully consistent with independent results of $g(\ell)$ calculated via thermodynamic integration; while an extra film-height dependence of the effective stiffness, $\gamma_{cws} = \gamma_\infty + \Delta\gamma(\ell)$, with $\Delta\gamma(\ell) \propto g''(\ell)$ holds for films up to a few molecular diameters thick.

Our simulations are performed for a well-known model of “Argon adsorbed on solid carbon dioxide” that was employed extensively in order to confirm the theoretical prediction of prewetting by Ebner and Saam.[19–21] Argon is described by means of a Lennard–Jones potential, with a well depth of ϵ and a molecular diameter of σ (henceforth employed as length unit). Note, however, that the fluid–fluid interactions are short range, since the Lennard–Jones potential is truncated beyond a distance of 2.5σ . The fluid interacts above the upper half plane $z > 0$ with a flat inert substrate exhibiting a truly long range potential of the form $V(z) = -H_w/z^3$, with H_w the Hamaker constant and z the perpendicular distance to the substrate.[22] This choice of interactions turns out to be of great advantage. On the one hand, we can exploit various mean field results that are known for systems with short-range fluid–fluid forces.[11, 12, 23–25] On the other hand, the long range external field amplifies the signature of capillary waves that would otherwise pass unnoticed. This will allow us to test predictions of relevance to short-range-wetting that have remained a matter of debate for many years.[11, 12]

We perform our study at a temperature $k_B T/\epsilon = 0.60$, just above the wetting transition (ca. $k_B T_w/\epsilon =$

0.598).[26, 27] Close to coexistence, an adsorbed film of liquid density, ρ_l , is found in equilibrium with a vapor phase, ρ_v . Direct measurements of the interface potential are obtained by performing grand canonical simulations and collecting the probability, $P(\Gamma)$ of finding a given adsorbed amount Γ of molecules.[22] Using the intrinsic sampling method (ISM),[28] an accurate technique for locating the interface of a corrugated film, we relate adsorption to average film thickness, ℓ . A coarse-grained interface potential is then estimated as $g(\ell) = -k_B T \ln P(\ell)$. [27, 29, 30]

In our system, the wetting temperature is very low, close to the fluid’s triple point. Hence, the density profile of a an adsorbed liquid film is dominated by a single relaxation mode with damped oscillatory behavior,[23] such that $\rho(z) = \rho_l [1 + h(z)]$, with $h(z) = A_w \cos(k_o z + \theta) e^{-b_o z}$. We checked that both the inverse correlation length b_o and the wave vector k_o are equal to those required to describe the oscillations of the bulk liquid correlation function (c.f. Fig.1), as expected for short-range fluids subject to an external field. Only the amplitude, A_w and phase θ of the oscillations are dictated by the external field.[24, 25, 31] The mean field interface potential emerging from this scenario may be split into intrinsic and external field contributions, $g(\ell) = g_{mb}(\ell) + g_V(\ell)$. The first term, $g_{mb}(\ell)$ is a highly non-trivial functional of the number density $\rho(z; \ell)$, and includes many-body fluid–fluid correlations. Whereas its structure may be quite complex, and could in principle pick up oscillatory behavior of the adsorbed layer it is expected to decay exponentially fast.[23] The second contribution,

$$g_V(\ell) = \int V(z) \rho(z; \ell) dz \quad (3)$$

stems from the wall–fluid external field and recovers the familiar long-range Hamaker dependence $g_V(\ell) \propto \ell^{-2}$.

The coarse grained interface potential that is obtained in our simulations is renormalized up to wavelengths equal to the lateral system dimensions, and shows no sign of oscillatory behavior (Fig.1). Rather, beyond about $\ell = 3\sigma$ it exhibits a monotonic decay that is usually attributed to long-range forces. The signature of layering is revealed only when we consider the derivatives of $g(\ell)$. Particularly, $g''(\ell)$, which we can evaluate numerically thanks to our highly accurate data (Fig.2) shows a clear oscillatory behavior superimposed on the expected long-range decay. In order to unravel the nature of these oscillations, we evaluated Eq. (3) numerically, using simulated density profiles for $\rho_\ell(z)$. The results are indistinguishable from the long-range Hamaker contribution $\approx \frac{1}{2} H_w \Delta\rho \ell^{-2}$ depicted as a dashed line in Fig.1. However, taking second derivatives, we observe once again a clear oscillatory behavior of $g''_V(\ell)$, that resembles the oscillations of $g''(\ell)$ appearing between about two and four σ (Fig.2). This shows that not only the decay of g'' , but also the oscillations are to a great extent due to the

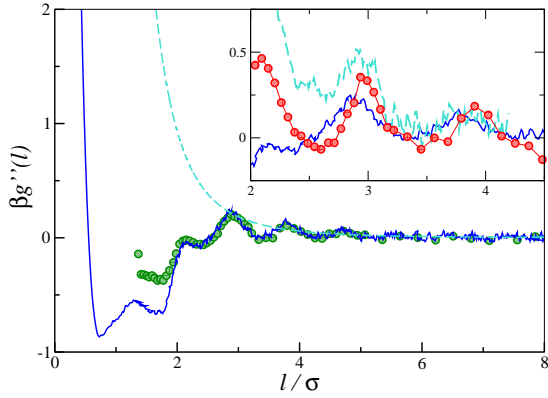


FIG. 2. Second derivative of the interface potential (full line) compared with expectations from the CWS, g''_{cws} (green circles) and from the Hamaker model (dashed line). Notice almost perfect match of g'' with g''_{cws} up to $\ell = 2\sigma$. Inset: Enlarged view of g'' (full line), as compared with g''_{cws} (dashed line) and $\gamma_{cws} - \gamma_\infty$ (symbols).

external field contribution.

Independent canonical simulations are carried out for adsorbed films ranging from one to about ten molecular diameters thick. For each configuration a film–height profile $\ell(\mathbf{x})$ is determined,[28] and the Fourier components $\ell_{\mathbf{q}}$ calculated. The thermal average $\langle |\ell_{\mathbf{q}}|^2 \rangle$ is fitted to a quadratic polynomial in q^2 , as suggested by expectations from Eq. (2), yielding independent estimates of g''_{cws} , γ_{cws} and κ_{cws} (Fig.2–3).

The results for g''_{cws} as obtained from the CWS, show an excellent agreement with independent estimates of g'' obtained from thermodynamic integration, for all film lengths up to 2σ (Fig.2). More impressively, the good agreement holds even in regions where $g'' < 0$. Previously, interface potentials in the unstable region have been estimated by studying the behavior of dewetting patterns.[32–34] Films with negative g'' are unstable to all perturbations beyond the critical wavelength $\lambda_c = 2\pi(\gamma_\infty/|g''|)^{1/2}$. [6, 33] Using $\beta\gamma_\infty = 1.66\sigma^{-2}$, [27] and the value of g'' at the second minima, where the agreement breaks down, we find that the onset of instability occurs for fluctuations of wavelength $\lambda_c \approx 10\sigma$. This is just about the lateral system size of our study, $L = 10\sigma$ and serves to motivate why we are able to equilibrate “unstable” films in our finite size simulations. Unfortunately, the cluster criteria required to define the Fourier modes $\ell_{\mathbf{q}}$ breaks down below $\ell = \sigma$, so that we are unable to compare g'' and g''_{cws} in this range.

According to Eq. (2), the first order coefficient in our fit to $1/\langle |\ell_{\mathbf{q}}|^2 \rangle$ yields an estimate of the stiffness. This expectation has been confirmed for a free liquid–vapor interface in several studies.[28, 35–38] In our adsorbed

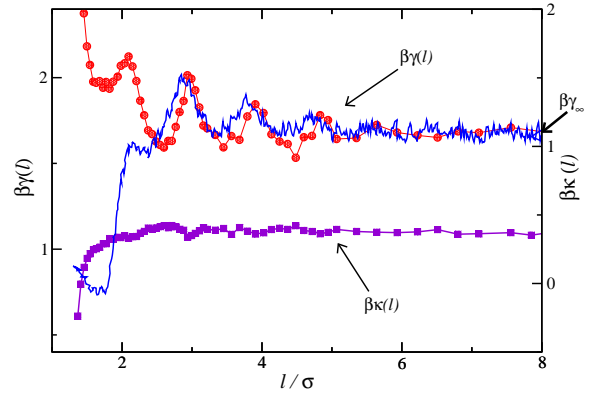


FIG. 3. Film–thick–dependent surface tension, $\gamma_{cws}(\ell)$ (circles, left axis) and bending rigidity κ_{cws} (squares, right axis) as obtained from the CWS. The full lines are predictions from the model $\gamma_\infty + g''(\ell)/b^2$, with $b = 0.85\sigma^{-1}$. The thick arrow points to the value of γ_∞ as obtained independently for the free interface.

films we find good agreement with independent measures of γ_∞ . [27] For films below about $\ell < 6\sigma$, however, γ_{cws} becomes film–thick dependent and picks up a strong oscillatory behavior vaguely resembling that of g'' (Fig.3). Our results show that, as opposed to γ_{cws} , the bending rigidity, κ_{cws} is rather insensitive to ℓ , remaining almost constant up to 2σ , where it strongly decreases and becomes negative (Fig.3) as the film becomes unstable (i.e., $g''(\ell) < 0$).

Here we would like to point out that the need for a film–thick dependent stiffness results naturally from an improved theory of capillary wave broadening incorporating distortions of the intrinsic density profile.

First we consider the liquid–vapor interface for an adsorbed film of infinite thickness, obeying a LGW density functional. We seek density profiles minimizing the free energy functional subject to the constraint, $\rho_{lv}(\mathbf{x}, z = \ell(\mathbf{x}); \Sigma) = \rho_{1/2}$, where $\rho_{1/2} = \frac{1}{2}(\rho_l + \rho_v)$ (crossing criterion) and Σ is shorthand for the functional dependence, $[\ell(\mathbf{x})]$. A general solution to this problem is not possible, but treating liquid and vapor branches of the density profile separately (double parabola approximation) leads to the following Helmholtz equation as the solution to the functional minimization:[11, 12]

$$\nabla^2 \Delta\rho_{lv}(\mathbf{r}; \Sigma) - b^2 \Delta\rho_{lv}(\mathbf{r}; \Sigma) = 0 \quad (4)$$

where $\Delta\rho_{lv}(\mathbf{r}; \Sigma) = \rho_{lv}(\mathbf{r}; \Sigma) - \rho_\infty$ is the density excess over the bulk value, ρ_∞ , we assume liquid (vapor) asymptotic densities to the left (right) of $z = \ell$, and b is the decay rate of the liquid–vapor interface. Considering an expansion of the density profile in transverse Fourier modes, $\Delta\rho_{lv}(z; \mathbf{q})e^{i\mathbf{q}\cdot\mathbf{x}}$, we find a general solution of the

form:

$$\rho_{lv}(\mathbf{r}; \Sigma) = \rho_\infty + \sum_{\mathbf{q}} A_{\mathbf{q}} e^{\pm b_{\mathbf{q}} z} e^{i\mathbf{q} \cdot \mathbf{x}} \quad (5)$$

where \pm indicates solutions for either the left (liquid) or right (vapor) half planes; while the eigenvalues $b_{\mathbf{q}} = \sqrt{b^2 + q^2}$ physically correspond to wave vector dependent inverse correlation lengths, that impose fast damping of the density perturbation for short wavelengths.

Now consider the liquid–vapor interface as it approaches the substrate. A smectic density wave of the form $\rho_l(1 + h(z))$ propagates from the wall outwards and perturbs the asymptotic liquid density, ρ_l . For thin films, the liquid–vapor interface feels the distortion, and is thus modulated by $h(z)$. Accordingly, we consider a *superposition model*, whereby the density profile of the adsorbed film results from the superposition of $h(z)$ onto $\rho_{lv}(\mathbf{r}; \Sigma)$, i.e., $\rho(\mathbf{r}; \Sigma) = [1 + h(z)]\rho_{lv}(\mathbf{r}; \Sigma)$. In order to obtain the Fourier coefficients, $A_{\mathbf{q}}$ of the distorted liquid–vapor interface, we evaluate $\rho(\mathbf{r}, \Sigma)$ at the boundary, $z = \ell(\mathbf{x})$. Assuming a flat interface, with $\ell(\mathbf{x}) = \ell$ everywhere, we readily obtain the zero order result for $A_{\mathbf{q}=0}$, which yields the following *intrinsic* density profile:

$$\rho_\pi(z; \ell) = [1 + h(z)] \left(\rho_\infty + \frac{\Delta\rho_{1/2} - \rho_\infty h(\ell)}{1 + h(\ell)} e^{\pm b(z-\ell)} \right) \quad (6)$$

This simple model already provides a rather good description of the average density profiles, $\rho(z; \ell)$ obtained from simulation (c.f Fig.1).

In order to assess the role of capillary waves we follow a procedure suggested by Tarazona,[39] first performing a Taylor expansion about deviations from a planar interface $\delta\ell(\mathbf{x}) = \ell(\mathbf{x}) - \ell$ and then Fourier transforming the resulting expression. Retaining terms up to order $|\delta\ell_{\mathbf{q}}|^2$, and integrating over \mathbf{x} , we find that the laterally averaged density profile, $\rho(z; \Sigma) = \langle \rho(\mathbf{r}; \Sigma) \rangle_{\mathbf{x}}$ may be written solely in terms of the intrinsic density profile as:

$$\rho(z; \Sigma) = \rho_\pi(z; \ell) + \frac{1}{2} \sum_{\mathbf{q}} \left[\frac{d^2 \rho_\pi(z)}{d\ell^2} \mp \frac{d\rho_\pi(z)}{d\ell} \frac{q^2}{b} \right] |\delta\ell_{\mathbf{q}}|^2 \quad (7)$$

This result features capillary wave broadening effects beyond the classical theory, which includes only the first two terms in the right hand side. Here we see that broadening of the profile is enhanced by terms $\langle (\frac{\nabla\ell}{b})^2 \rangle_x$ that account for distortion of the profile due to curvature of the interface.

In order to understand the significance of this contribution most easily, it is convenient to consider the limit of thick films, where $d^2 \rho_\pi(z)/d\ell^2$ and $\mp b d\rho_\pi(z)/d\ell$ become identical in the double parabola approximation. Substitution of Eq. (7) into Eq. (3), immediately yields the following external field contribution to the interface po-

tential,

$$g_V(\Sigma) = g_V(\ell) + \frac{1}{2} g_V''(\ell) \sum_{\mathbf{q}} \left(1 + \frac{q^2}{b^2} \right) |\delta\ell_{\mathbf{q}}|^2 \quad (8)$$

thus, the enhanced broadening of the density profile results in an extra contribution of order q^2 that is absent in the classical theory.

Employing this result for the interface potential in Eq. (1), we find that the CWS must now take the form:

$$\frac{k_B T}{A \langle |\ell_{\mathbf{q}}|^2 \rangle} = g''(\ell) + \left(\gamma_\infty + \frac{g_V''(\ell)}{b^2} \right) q^2 \quad (9)$$

i.e., the distortion of the density profile due to capillary waves couples $g_V(\ell)$ with terms of order q^2 , effectively providing a film–thick–dependent surface tension. According to our analysis, the ℓ dependence will closely follow $g''(\ell)$ as long as the film is thick enough and the interface potential is dominated by the external field contribution. Particularizing Eq. (8) and Eq. (9) for wall–fluid interactions with algebraic decay our results are exactly as obtained previously from the nonlocal theory of interfaces,[13] and thus lend support to the nonlocal theory of short–range–wetting.[12]

We do not expect this simplified treatment to provide a quantitative description of our simulations since i) the fluid actually has different correlation lengths for the liquid and vapor phases and ii) the superposition model does not accurately describe the density derivatives of the film profile with respect to ℓ . However, we can test the predictions for $\gamma_{cws} \approx \gamma_\infty + g''(\ell)/b^2$, using our independent results for γ_∞ and $g''(\ell)$, and considering b as an effective inverse correlation length. Surprisingly, a test of this hypothesis provides good agreement for films of thickness down to $\ell = 2.5\sigma$, where $h(z)$ is still far from having decayed (Fig.3). Interestingly, the steep increase of $\gamma_{cws}(\ell)$ below $\ell_0 = 2.5\sigma$, which is not captured by the full $g''(\ell)$, rather obeys qualitatively the trend followed by $g_V''(\ell)$ as obtained from integration of Eq. (3) (Fig.1).

The significance of the effective surface tension may be readily understood in terms of the parallel correlation length, which is defined in the classical theory as $\xi_{\parallel}^2 = \gamma_\infty/g''(\ell)$. Using instead the effective surface tension we find that $\xi_{\parallel}^2 = \gamma_\infty/g''(\ell) + \xi_b^2$, where ξ_b is the bulk correlation length. As the classical result may become small either close to a critical point or under a strong field, our improvement merely provides the fairly obvious requirement of a lower bound ξ_b to ξ_{\parallel} . This expectation may be assessed experimentally for a free fluid–fluid interface under the gravitational field, since then $\xi_{\parallel}^2 = a^2 + \xi_b^2$, with a the capillary length. A colloid/polymer suspension close to the fluid–fluid consolute point seems an excellent candidate for experimental verification.[40]

In summary, we have demonstrated that capillary wave fluctuations of thick adsorbed liquid films obey expecta-

tions from classical capillary wave theory. For thin films, however, a hitherto unnoticed capillary wave broadening mechanism results in an effective film-thickness-dependent surface tension. This observation has important implications in both the structure and dynamics of adsorbed condensates.

LGM would like to thank P. Tarazona for helpful discussions and critical reading of the manuscript as well as E. M. Fernández and E. Chacón for invaluable assistance with the ISM. We also wish to thank R. Evans, A. Parry, S. Dietrich, N. Bernardino, V. Martín-Mayor and A. Rodríguez-Bernal for helpful discussions. We acknowledge financial support from grant FIS2010-22047-C05-05 of the Spanish Ministerio de Economía y Competitividad, and project P2009/ESP/1691 (MODELICO) from Comunidad Autónoma de Madrid.

-
- [1] M. A. Burns, C. H. Mastrangelo, T. S. Sammarco, F. P. Man, J. R. Webster, B. N. Johnson, B. Foerster, D. Jones, Y. Fields, A. R. Kaiser, and D. T. Burke, *Proc. Nat. Acad. Sci.* **93**, 5556 (1996).
- [2] R. Seemann, M. Brinkmann, E. J. Kramer, F. F. Lange, and R. Lipowsky, *Proc. Nat. Acad. Sci.* **102**, 1848 (2005).
- [3] S. Dietrich, in *Phase Transitions and Critical Phenomena*, Vol. 12, edited by C. Domb and J. L. Lebowitz (Academic, New York, 1988) pp. 1–89.
- [4] M. Schick, in *Liquids at Interfaces*, Les Houches Lecture Notes (Elsevier Science Publishers, Amsterdam, 1990) pp. 1–89.
- [5] F. P. Buff, R. A. Lovett, and F. H. Stillinger, *Phys. Rev. Lett.* **15**, 621 (1965).
- [6] A. Vrij, *Discuss. Faraday Soc.* **42**, 23 (1966).
- [7] D. S. Fisher and D. A. Huse, *Phys. Rev. B* **32**, 247 (1985).
- [8] P. G. de Gennes, F. Brochard-Wyart, and D. Quéré, *Capillarity and Wetting Phenomena* (Springer, New York, 2004).
- [9] H. T. Dobbs and J. O. Indekeu, *Physica. A* **201**, 457 (1993).
- [10] P. Upton, *Int. J. Thermophys.* **23**, 1 (2002).
- [11] A. J. Jin and M. E. Fisher, *Phys. Rev. B* **47**, 7365 (1993).
- [12] A. O. Parry, C. Rascón, N. R. Bernardino, and J. M. Romero-Enrique, *J. Phys.: Condens. Matter* **18**, 6433 (2006).
- [13] N. R. Bernardino, A. O. Parry, C. Rascón, and J. M. Romero-Enrique, *Journal of Physics: Condensed Matter* **21**, 465105 (2009).
- [14] I. M. Tidswell, T. A. Rabedeau, P. S. Pershan, and S. D. Kosowsky, *Phys. Rev. Lett.* **66**, 2108 (1991).
- [15] A. K. Doerr, M. Tolan, W. Prange, J.-P. Schlomka, T. Seydel, W. Press, D. Smilgies, and B. Struth, *Phys. Rev. Lett.* **83**, 3470 (1999).
- [16] J. Rowlinson and B. Widom, *Molecular Theory of Capillarity* (Clarendon, Oxford, 1982).
- [17] K. R. Mecke and S. Dietrich, *Phys. Rev. E* **59**, 6766 (1999).
- [18] E. M. Fernández, E. Chacón, and P. Tarazona, *Phys. Rev. B* **86**, 085401 (2012).
- [19] J. E. Finn and P. A. Monson, *Mol. Phys.* **65**, 1345 (1988).
- [20] S. Sokolowski and J. Fischer, *Phys. Rev. A* **41**, 6866 (1990).
- [21] C. Ebner and W. F. Saam, *Phys. Rev. Lett.* **38**, 1486 (1977).
- [22] “See supplemental material at [url will be inserted by publisher] for [model and simulation details].”
- [23] A. A. Chernov and L. V. Mikheev, *Phys. Rev. Lett.* **60**, 2488 (1988).
- [24] R. Evans, R. J. F. L. de Carvalho, J. R. Henderson, and D. C. Hoyle, *J. Chem. Phys.* **100**, 591 (1994).
- [25] J. R. Henderson, *Phys. Rev. E* **50**, 4836 (1994).
- [26] J. R. Errington, *Langmuir* **20**, 3798 (2004).
- [27] R. de Gregorio, J. Benet, N. A. Katcho, F. J. Blas, and L. G. MacDowell, *J. Chem. Phys.* **136**, 104703 (2012).
- [28] P. Tarazona and E. Chacón, *Phys. Rev. B* **70**, 235407 (2004).
- [29] L. G. MacDowell and M. Müller, *J. Chem. Phys.* **124**, 084907 (2006).
- [30] L. G. MacDowell, *Euro. Phys. J. ST* **197**, 131 (2011).
- [31] S. H. L. Klapp, Y. Zeng, D. Qu, and R. von Klitzing, *Phys. Rev. Lett.* **100**, 118303 (2008).
- [32] H. I. Kim, C. M. Mate, K. A. Hannibal, and S. S. Perry, *Phys. Rev. Lett.* **82**, 3496 (1999).
- [33] R. Seemann, S. Herminghaus, and K. Jacobs, *Phys. Rev. Lett.* **86**, 5534 (2001).
- [34] A. R. Herring and J. R. Henderson, *J. Chem. Phys.* **132**, 084702 (2010).
- [35] M. Müller and M. Schick, *J. Chem. Phys.* **105**, 8885 (1996).
- [36] M.-D. Lacasse, G. S. Grest, and A. J. Levine, *Phys. Rev. Lett.* **80**, 309 (1998).
- [37] A. Milchev and K. Binder, *Europhys. Lett* **59**, 81 (2002).
- [38] R. L. C. Vink, J. Horbach, and K. Binder, *J. Chem. Phys.* **122**, 134905 (2005).
- [39] P. Tarazona, private communication.
- [40] D. G. Aarts, M. Schmidt, and H. N. K. Lekkerkerker, *Science* **304**, 847 (2004).